A LETTERS JOURNAL EXPLORING THE FRONTIERS OF PHYSICS

Società Italiana di Fisica

edp sciences IOP Institute of Physics

LETTER

Dynamical thermalization in isolated quantum dots and black holes

To cite this article: Andrey R. Kolovsky and Dima L. Shepelyansky 2017 *EPL* **117** 10003

View the article online for updates and enhancements.

Related content

- Dynamical thermalization of Bose-Einstein condensate in Bunimovich stadium
  L. Ermann, E. Vergini and D. L. Shepelyansky
- Quantum Gibbs distribution from dynamical thermalization in classical nonlinear lattices
  Leonardo Ermann and Dima L Shepelyansky
- LSD for conservative system of coupled quantumstates
  V S Starovoitov

Recent citations

- Symmetry Breaking in Coupled SYK or Tensor Models
  Jaewon Kim *et al*
- Dynamical decoherence of a qubit coupled to a quantum dot or the SYK black hole
  Klaus M. Frahm and Dima L. Shepelyansky
- Strongly Correlated Metal Built from Sachdev-Ye-Kitaev Models
  Xue-Yang Song *et al*

IOP ebooks™

Bringing together innovative digital publishing with leading authors from the global scientific community.

Start exploring the collection–download the first chapter of every title for free.

This content was downloaded from IP address 84.237.90.20 on 07/09/2020 at 14:14

A Letters Journal Exploring the Frontiers of Physics

January 2017

EPL, **117** (2017) 10003
doi: 10.1209/0295-5075/117/10003

www.epljournal.org

Dynamical thermalization in isolated quantum dots and black holes

Andrey R. Kolovsky[1,2] and Dima L. Shepelyansky[3]

[1] *Kirensky Institute of Physics - 660036 Krasnoyarsk, Russia*
[2] *Siberian Federal University - 660041 Krasnoyarsk, Russia*
[3] *Laboratoire de Physique Théorique du CNRS (IRSAMC), Université de Toulouse, UPS F-31062 Toulouse, France*

received 20 December 2016; accepted in final form 2 February 2017
published online 20 February 2017

PACS 05.45.Mt – Quantum chaos; semi-classical methods
PACS 04.60.-m – Quantum gravity
PACS 78.67.Hc – Quantum dots

Abstract – We study numerically a model of quantum dot with interacting fermions. At strong interactions with small conductance the model is reduced to the Sachdev-Ye-Kitaev black-hole model while at weak interactions and large conductance it describes a Landau-Fermi liquid in a regime of quantum chaos. We show that above the Åberg threshold for interactions there is an onset of dynamical themalization with the Fermi-Dirac distribution describing the eigenstates of an isolated dot. At strong interactions in the isolated black-hole regime there is also the onset of dynamical thermalization with the entropy described by the quantum Gibbs distribution. This dynamical thermalization takes place in an isolated system without any contact with a thermostat. We discuss the possible realization of these regimes with quantum dots of 2D electrons and cold ions in optical lattices.

Copyright © EPLA, 2017

Introduction. – Recently it has been shown that there is a duality relation between an isolated quantum dot with infinite-range strongly interacting fermions and a quantum black-hole model in $1 + 1$ dimensions [1–3]. This system, called the Sachdev-Ye-Kitaev (SYK) model, attracted great interest of the quantum gravity community (see, *e.g.*, [4–7]). A possible realization of the SYK model with ultracold atoms in optical lattices has been proposed recently in [8]. An important element of the SYK model is an emergence of many-body quantum chaos with a maximal Lyapunov exponent for dynamics in a semiclassical limit [5,9].

It should be noted that in fact the SYK model first appeared in the context of nuclear physics where the strongly interacting fermions had been described by the two-body random interaction model (TBRIM) with all random two-body matrix elements between fermions on degenerate energy orbitals [10–13]. The majority of the matrix elements of the TBRIM Hamiltonian is zero since the two-body interactions impose selective transition rules. Thus, this case is rather different from the case of the random matrix theory (RMT) introduced by Wigner for the description of complex nuclei, atoms and molecules [14,15]. In spite of this difference, it had been shown that the level spacing statistics $P(s)$ in TBRIM is described by the Wigner-Dyson distribution $P_W(s)$ typical for the RMT [11,13]. A similar situation appeared later for the models of quantum chaos also characterized by sparse matrices being rather far from the RMT type but also characterized by the Wigner-Dyson statistics for matrices of a specific symmetry class [16–18]. The validity of RMT for the SYK model at different symmetries has been demonstrated in the recent fundamental and detailed studies reported in [19]. Transport properties of SYK and its extensions have also been discussed recently [20].

In this letter we present the studies of the SYK-type model extending parallels between physics of quantum dots and black holes. Indeed, the TBRIM and SYK systems have degenerate non-interacting orbitals while for quantum dots it is natural to have non-degenerate orbitals characterized by a certain average one-particle level spacing Δ. This spacing Δ can be much smaller than a typical interaction strength U between fermions and then we have the usual SYK or TBRIM degenerate regime ($\Delta \ll U$). In the opposite limit we have the regime of weak interactions typical for metallic dots ($\Delta \gg U \approx \Delta/g$) where the

interaction is determined by a dimensionless dot conductance $g = E_c/\Delta$ with E_c being the Thouless energy [21,22]. Even if the average spacing between excited levels drops exponentially with the number of fermions, the mixing of levels takes place only at interactions U being much larger than this spacing since the two-body selection rules connect directly only a polynomial number of states. The border for the emergence of the RMT $P_W(s)$ statistics is determined by the Åberg criterion [23,24] telling that the transition to RMT takes place when the average two-body matrix elements become larger than the average spacing between directly coupled states. This criterion has been confirmed in extensive numerical simulations with interacting fermions and spin systems [25–28]. Thus, at $g \gg 1$ the RMT statistics appears only for relatively high excitation above the quantum dot Fermi energy E_F [23–25]:

$$\delta E = E - E_F > \delta E_{ch} \approx g^{2/3}\Delta. \qquad (1)$$

This border is in good agreement with the spectroscopy experiments of individual mesoscopic quantum dots [29]. Of course, an exact check of the Åberg criterion via numerical simulations is not an easy task since the matrix size grows exponentially with the number of fermions. Thus, the validity of the Åberg border (1) is still under active discussions in relation to the many-body localization-delocalization (MBL) transition (see [30,31] and references therein). We also note that the quantum chaos and RMT statistics in the interacting Bose systems has been studied in [32].

In fact the border (1) assumes also that the emergence of RMT statistics appears as a result of the onset of quantum ergodicity which, in its turn, leads to a dynamical thermalization in an isolated system [25]. Thus, the relation (1) is based on a rather general dynamical thermalization conjecture (DTC). According to the DTC individual eigenstates of an isolated system are described by the standard Fermi-Dirac thermal distribution. The examples of thermalized individual eigenstates have been presented in [27]. This individual eigenstate thermalization is more striking than the thermal distribution of probabilities averaged over a group of eigenstates which had been seen earlier in the numerical simulations of TBRIM with $\Delta > U$ [33]. At present, the dynamical thermalization of individual eigenstates is known as the eigenstate thermalization hypothesis (ETH) and attracts great interest of the scientific community (see, *e.g.*, [34–36]).

The direct check of DTC from the filling factors of one-particle orbitals is possible but it requires diagonalization of large matrices and still the fluctuations are significant even for sizes $N \sim 10^7$ (see, *e.g.*, fig. 6 in [27]). In fact it has been found that the fluctuations are significantly reduced if we determine numerically the dependence of entropy S on energy E computed for individual eigenstates. The reduction of fluctuations is due to the fact that both S and E are extensive self-averaging characteristics. The numerically obtained dependence $S(E)$ can be directly compared with those of the theoretical Fermi-Dirac or Bose-Einstein distributions [37]. The power of this approach for a verification of DTC has been confirmed in the numerical simulations of classical nonlinear disordered chains [38], the Gross-Pitaevski equation for the Bose-Einstein condensate in chaotic billiards [39,40] and quantum many-body Bose-Hubbard rings with disorder [41]. Here we use this approach for the investigation of dynamical thermalization in isolated quantum dots and black holes described by TBRIM and SYK-type models.

Model description. – The model is described by the Hamiltonian for L spin-polarized fermions on M energy orbitals ϵ_k ($\epsilon_{k+1} \geq \epsilon_k$):

$$\widehat{H} = \widehat{H}_0 + \widehat{H}_{int}, \quad \widehat{H}_0 = \frac{1}{\sqrt{M}} \sum_{k=1}^{M} v_k \hat{c}_k^\dagger \hat{c}_k,$$
$$\widehat{H}_{int} = \frac{1}{\sqrt{2M^3}} \sum_{ijkl} J_{ij,kl} \hat{c}_i^\dagger \hat{c}_j^\dagger \hat{c}_k \hat{c}_l. \qquad (2)$$

Here the fermion operators $\hat{c}_i^\dagger, \hat{c}_i$ satisfy the usual anti-commutation relation. The interaction matrix elements $J_{ij,kl}$ are random complex variables with a standard deviation J and zero average value. The interacting part $\widehat{H}_{int}$ is the same as those used in [8] (see eq. (1) there). As in [8] we consider the model with complex fermions (complex matrix elements $J_{ij,kl}$) [3] which is slightly different from the case with real fermions (real $J_{ij,kl}$) [2]. However, in our model (2), in addition to the interaction Hamiltonian $\widehat{H}_{int}$, there is also the unperturbed part $\widehat{H}_0$ describing one-particle orbitals $\epsilon_k = v_k/\sqrt{M}$ in a quantum dot of non-interacting fermions. The average of one-orbital energies is taken to be $\overline{v_k^2} = V^2$ with $\overline{v_k} = 0$. Thus, the unperturbed one-particle energies ϵ_k are distributed in an energy band of size V and the average level spacing between them is $\Delta \approx V/M^{3/2}$, while the two-body coupling matrix element is $U \approx J/M^{3/2}$. Hence, in our model the effective dimensionless conductance in (1) is $g = \Delta/U \approx V/J$. The total matrix size of the Hamiltonian (2) is $N = M!/L!(M-L)!$ and each multi-particle state is coupled with $K = 1+L(M-L)+L(L-1)(M-L)(M-L-1)/4$ states [25,33,36]. Here we consider the case of approximate half-filling with $L \approx M/2$.

Dynamical thermalization ansatz. – We start from the case of $g \gg 1$ when one-particle orbitals are well defined. If the DTC is valid, then weak or moderate interactions should lead to the standard Fermi-Dirac thermal distribution over M one-particle orbitals with energies ϵ_k and filling factors [37]:

$$n_k = \frac{1}{e^{\beta(\epsilon_k - \mu)} + 1}, \qquad \beta = 1/T, \qquad (3)$$

with the chemical potential μ determined by the conservation of number of fermions $\sum_{k=1}^{M} n_k = L$. Then following [37], at a given temperature T, the system energy E

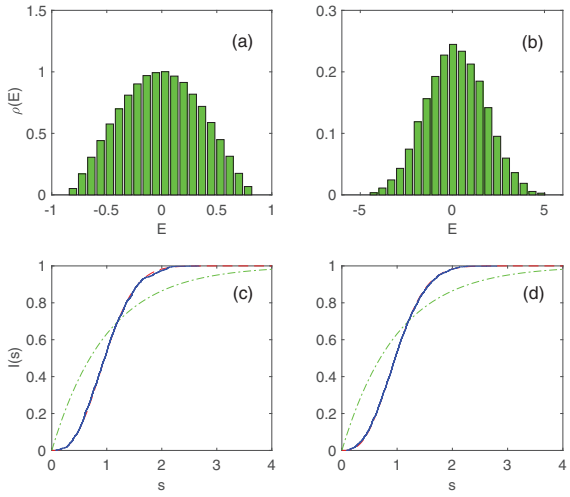

Fig. 1: (Color online) Top row: density of states $\rho(E) = \mathrm{d}N(E)/\mathrm{d}E$ for the model (2). Bottom row (c), (d): integrated level spacing statistics $I(s) = \int_0^s \mathrm{d}s' P(s')$ for the Poisson statistics $P_P(s)$ (dashed green curve), for the Wigner surmise $P_W(s)$ (dashed red curve) and numerical data $P(s)$ for the central energy region comprising 80 percent of the states (blue curve, almost superposed with the red dashed curve). Here $M = 14, L = 6, N = 3003$, and $J = 1, V = 0$ ((a), (c)) and $J = 1, V = \sqrt{14}$ ((b), (d)).

and von Neumann entropy S are given by

$$E(T) = \sum_{k=1}^{M} \epsilon_k n_k, \qquad S(T) = -\sum_{k=1}^{M} n_k \ln n_k. \qquad (4)$$

The Fermi gas entropy is $S_F = -\sum_{k=1}^{M}(n_k \ln n_k + (1 - n_k)\ln(1-n_k))$ [37]. The relations (3), (4) determine an implicit functional dependence $S(E)$ which is very convenient for numerical checks since both quantities S and E are extensive and self-averaging. The numerical computation of S and E from the eigenstates ψ_m and eigenenergies E_m of H is straightforward by using $n_k(m) = \langle\psi_m|\hat{c}_k^\dagger \hat{c}_k|\psi_m\rangle$. With (4) this gives the entropy S_m of the eigenstate ψ_m.

Of course, the DTC is based on a quantum ergodicity of eigenstates that can appear only in the regime of Wigner-Dyson statistics $P_W(s) = 32\,\mathrm{s}^2 \exp(-4\,\mathrm{s}^2/\pi)/\pi^2$ (Wigner surmise corresponding to the Gaussian unitary ensemble (GUE) symmetry of our model). Indeed, in the absence of ergodicity the statistics is described by the Poisson distribution $P_P(s) = \exp(-s)$ of independent uncorrelated eigenenergies. As usual, here the level spacing s, between adjacent eigenenergies E_m, E_{m+1} of the whole system, is measured in units of average level spacing assuming spectrum unfolding [17,18]).

Indeed, our results, presented in fig. 1, show that the RMT is valid for the SYK black-hole regime ($g = V/J \ll 1$) and for the quantum dot regime ($g = V/J > 1$) when the relation (1) is satisfied. We note that the Wigner-Dyson statistics at $V = 0$ had been also obtained in [11,13,19] for corresponding symmetries.

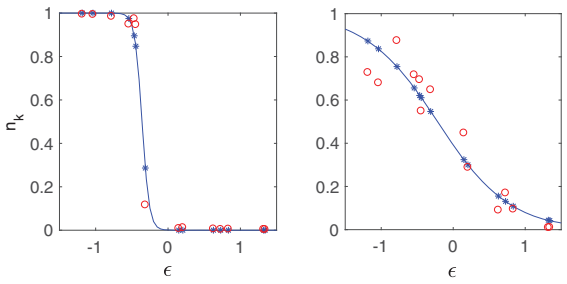

Fig. 2: (Color online) Dependence of filling factors n_k on energy ϵ for individual eigenstates obtained from exact diagonatization of (2) (red circles) and from the Fermi-Dirac ansatz with one-particle energy ϵ (3) (full blue curve; blue stars are shown at one-particle energy positions $\epsilon = \epsilon_k$). Here $M = 14, L = 6, N = 3003$, $J = 1, V = \sqrt{14}$ and eigenenergies (2) are $E = -4.4160$ (left panel), -3.0744 (right panel); the theory blue curves (3) are drawn for the temperatures corresponding to these energies $\beta = 1/T = 20$ (left panel), 2 (right panel), see fig. 3(b) below.

For the parameters of fig. 1 (right column) we indeed find that the DTC provides a good description of filling factors in agreement with (3) as is shown for two specific eigenstates in fig. 2. However, the fluctuations are significant and also the DTC should be verified for all eigenstates at a given set of parameters. Due to that we test the DTC validity using the approach developed for bosons in [39–41] based on the numerical computation of the dependence $S(E)$ from eigenstates of the Hamiltonian (2).

Quantum dot regime. – First of all we remark that, since the energy spectrum of our system (2) is inside a finite energy band, it is possible to have also negative temperatures for energies being in the upper half of the energy band. Such a regime of negative temperatures is well known for spin systems [42]. The relation between the temperature T and the energy E and the dependence of the chemical potential μ on T, obtained from the Fermi-Dirac ansatz (3), are shown in fig. 3. The center of the energy band at $E = 0$ corresponds to infinite temperature and $\beta = 0$. Here the entropy takes its maximal value $S(E = 0) = -L\ln(L/M)$ corresponding to equipartition of L fermions over M orbitals. With the increase of $|\beta|$ the entropy obviously decreases towards zero, which corresponds to the unit filling factor for L lowest ($T = +0$) or highest ($T = -0$) energy orbitals.

The dependence $S(E)$ for DTC in the quantum dot regime at $g = V/J > 11$, is shown in figs. 4(a)–(c). Here the conductance of the dot is not very large ($g = V/J \approx 3.7$) and practically all eigenstates are well thermalized with numerical points following the DTC theoretical curve. This is in agreement with the estimate (1) which gives the thermalization at rather low energy excitation $\delta E \approx 0.17$. In contrast, for $J = 0.1$ (panel (d)) we have a significant increase of $g = 37$ with a larger border for the RMT statistics $\delta E \approx 0.8$. As a result the numerical data have entropy S significantly below the theoretical value.

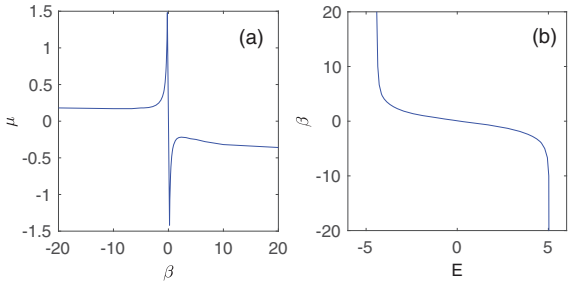

Fig. 3: (Color online) Dependence of the inverse temperature $\beta = 1/T$ on energy E (right panel) and chemical potential μ on β (left panel) given by the Fermi-Dirac ansatz (3) for the set of one-particle energies ϵ_k as in fig. 2.

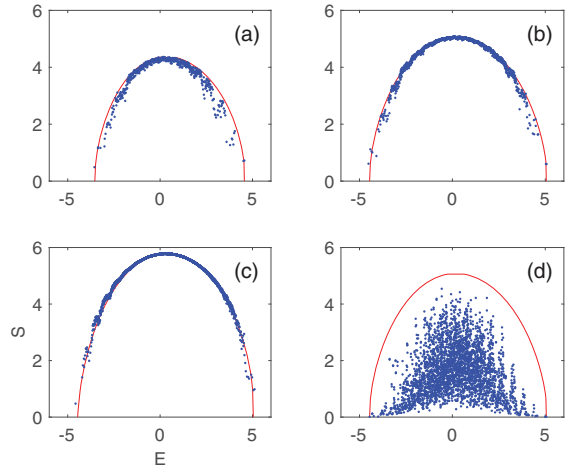

Fig. 4: (Color online) Dependence of the entropy on energy $S(E)$ for (a) $M = 12$, $L = 5$, $N = 792$, $J = 1$; (b) $M = 16$, $L = 7$, $N = 3003$, $J = 1$; (c) $M = 14$, $L = 6$, $N = 11440$, $J = 1$; (d) $M = 16$, $L = 7$, $N = 3003$, $J = 0.1$. Blue points show the numerical data E_m, S_m for all eigenstates, the red curves show the theoretical Fermi-Dirac thermal distribution (3). Here $V = \sqrt{14}$.

For each eigenstate with eigenenergy E it is possible to determine the occupation probabilities $n_k(E)$ on one-particle orbitals with orbital energies ϵ_k. In the DTC regime the dependence $n_k(E)$ is given by the Fermi-Dirac distribution (3) shown in fig. 5 (bottom left panel). The numerically obtained values $n_k(E)$, shown in fig. 5 (bottom right panel), demonstrate good agreement with the theory (3). This confirms the validity of the DTC for practically all eigenstates in the quantum dots with moderate values of conductance ($g = 4$ in fig. 5).

Here we presented results for one specific disorder realization. Similar results have been obtained for other disorder realizations. However, we do not present averaging over disorder since it is much more striking that the dynamical thermalization takes place even for one specific quantum dot with a given disorder realization.

SYK black-hole regime. – This regime corresponds to $g = V/J \ll 1$. In this case we find rather different

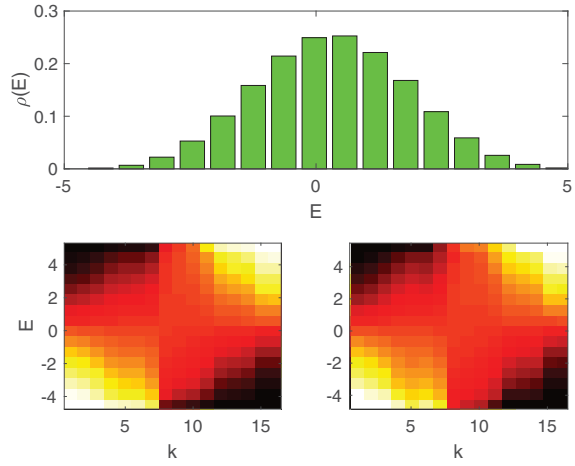

Fig. 5: (Color online) Top panel: dependence of the normalized density of states $\rho(E)$ on energy E ($\int \rho(E)\mathrm{d}E = 1$), $\rho(E)$ is averaged inside each energy cell. Bottom panels: occupation probabilities $n_k(E)$ of one-particle orbitals ϵ_k given by the theoretical Fermi-Dirac distribution (3) in the left panel, and by their numerical values obtained by exact diagonalization of (2) in the right panel; n_k is averaged over all eigenstates inside a given energy cell. The color changes from black for $n_k = 0$ via red, yellow to white for $n_k = 1$; orbital number k and eigenenergy E are shown on the x and y axes, respectively. Here $M = 16, L = 7, N = 11440, V = 4, J = 1$.

dependence $S(E)$ shown in fig. 6 (left panel) for several system sizes. In fact, here the entropy has its maximal value $S = -L\ln(L/M) \approx L\ln 2$ remaining practically independent of energy E in a broad energy interval in the center of the energy band. Only at the spectrum edges there is a small decrease of the entropy approximately by 10% of its maximal value. Here, as before, the values of S are obtained from n_k filling factors computed numerically from eigenstates ψ_m of (2) by their projection on non-interacting orbitals of H_0. The obtained dependence $S(E)$ is in a striking contrast with those of the quantum dot regime shown in the right panel of fig. 6 for comparison.

The fact that in the SYK model the entropy is practically independent of the energy E is not so surprising: the interactions are much stronger than the energies of one-particle orbitals so that many-body eigenstates are spread over all orbitals giving for them almost constant filling factors n_k and, hence, a constant entropy.

The distinguished feature of the SYK model is the absence of quasi-particles with natural orbital energies so that it is not possible to use the Fermi-Dirac ansatz (3) which worked so well for the quantum dot regime. Thus, to handle this case in the spirit of DTC we assume that there are some hidden quasi-particles which have certain one-particle orbitals ϵ_k and relatively weak interactions. For unknown ϵ_k values we require that the many-body density of states $\rho(E)$ found numerically at $V = 0$ is reproduced by many-body eigenenergies of non-interacting fermions located on ϵ_k orbitals (see, *e.g.*, fig. 1(a)). As

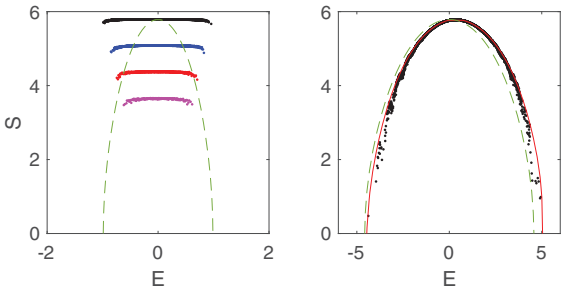

Fig. 6: (Color online) Dependence $S(E)$ for the SYK black-hole regime at $V = 0$ (left panel) and the quantum dot regime $V = \sqrt{14}$ (right panel). Here $M = 16, L = 7, N = 11440$ (black points), $M = 14, L = 6, N = 3003$ (blue points), $M = 12, L = 5, N = 792$ (red points), $M = 10, L = 4, N = 210$ (magenta points); in all cases $J = 1$. Points show numerical data E_m, S_m for all eigenstates, the full red curve shows the theoretical Fermi-Dirac distribution (3) in the right panel. Dashed gray curves in both panels show the Fermi-Dirac distribution (3) for a semi-empirical model of non-interacting quasi-particles for the case of black points (see text).

a first approximation we take equidistant values ϵ_k in a certain interval so that minimal and maximal energies of many-body Hamiltonian (2) at $V = 0$ are $E_{min} = \sum_{k=1}^{L} \epsilon_k$ and $E_{max} = \sum_{k=M-L}^{M} \epsilon_k$ with equidistant ϵ_k values. Then with these ϵ_k values and the Fermi-Dirac ansatz (3), (4) we find that the many-body density of states $\rho(E)$, obtained from the exact diagonalization of (2), is well reproduced. Such an approach can be applied both with well-defined quasi-particles ($g > 1$) and hidden quasi-particles ($g \ll 1$). The obtained $\rho(E)$ is not sensitive to a randomization of ϵ_k at the fixed energy range (E_{min}, E_{max}).

The obtained dependence $S(E)$ is shown in fig. 6 (right panel) for the quantum dot regime and we see that such a semi-empirical dashed gray curve is rather close to the theoretical distribution (3) obtained with one-particle orbitals at $g = 3.74$. Thus, we find that this semi-empirical approach works well in the regime $g > 1$. The semi-empirical results for the SYK black hole are shown in fig. 6 (left panel, dashed gray curve). Here the semi-empirical curve correctly describes the maximal value of S at $E \approx 0$ but it does not reproduce the large plateau obtained with numerical data from $n_k = \langle \psi_m | \hat{c}_k^\dagger \hat{c}_k | \psi_m \rangle$ and (4). We explain this difference by the fact that $\hat{c}_k^\dagger, \hat{c}_k$ operators are written in the initial degenerate basis with $\epsilon_k = v_k/\sqrt{M} = 0$. This original basis does not correspond to the basis and energies of hidden quasi-particles which are non-degenerate. We expect that a certain linear transformation can create a basis of new hidden quasi-particles with the filling factors that give the curve $S(E)$ being close to the semi-empirical curve in fig. 6 (left panel). However, the determination of such a basis remains a further challenge.

For the SYK model we obtain numerically that the entropy of the ground state is approximately $S(T = 0) \approx L \ln 2 \approx 0.69L$ corresponding to our approximate half-filling $L/M \approx 0.5$ with $n_k \approx 1/2$ and $S_F \approx 2S \approx 2L \ln 2$. This S_F value also corresponds to the logarithm of quantum number of states $N = (2L)!/[L!]^2$ at half-filling $L \approx M/2$. The $S(T = 0)$ value is approximately by a factor 3 larger than the numerical value $S(T = 0) = 0.21L$ obtained in [19] which is close to the theoretical value $S(T = 0) = 0.23L$ obtained in [5] for the Majorana SYK model [2] (there the number of states is $2^{L/2}$ that gives a simple states count entropy $S(T = 0) = (L/2) \ln 2 \approx 0.34L$ which differs from the final theoretical value $0.23L$ due to interaction effects). We note that the maximal entropy value, obtained in [8] for complex fermions, is close to the value we find here $S = L \ln 2$.

For the quantum dot regime a direct comparison of numerical n_k values with the theoretical Fermi-Dirac distribution (3) is possible as is shown in figs. 2 and 5. A determination of n_k values hidden quasi-particles in the SYK regime remains an open problem. We note that, in a certain sense, the thermodynamic computations done in [8,19] assume the thermal distribution over many-body levels E_m produced by a certain thermostat with temperature T being in contact with the quantum dot or the SYK black hole. We think that a bath thermostat is not realistic for the case of black holes which are well-isolated objects (at least in a first approximation). At the same time the DTC is well defined for isolated systems.

Discussion. – We demonstrate that the dynamical thermalization takes place for interacting fermions in a quantum dot for interactions being above a certain threshold. We argue that this threshold is given by the Åberg criterion (2) [23–25]. Above the threshold we directly show that the DTC is valid and the eigenstates of the many-body Hamiltonian (2) are described by the Fermi-Dirac thermal distribution (3) over one-particle orbitals in the quantum dot regime ($g = V/J > 1$). For the SYK black-hole regime with the DTC we reproduce the maximal entropy values and argue that hidden quasi-particle states reproduce the dependence of entropy S on energy E. We show that the verification of the DTC validity is done in a most optimal way by the comparison of the numerically obtained entropy on the energy dependence $S(E)$ with the theoretical Fermi-Dirac distribution (3) in the quantum dot regime and in the SYK black-hole case where the semi-empirical quasi-particle basis is still to be found. We point out that in previous studies [8,19] the thermodynamic characteristics have been obtained in an assumption of a contact between the system and an external bath thermostat that is opposite to the dynamical thermalization concept.

Even if we are not able to find suitable quasi-modes for the SYK regime at $g \ll 1$ we think that the problem risen here about the dynamical thermalization of a black hole and the validity of DTC (or ETH) for isolated black holes is important for the further understanding of quantum black holes. Indeed, in a good approximation a

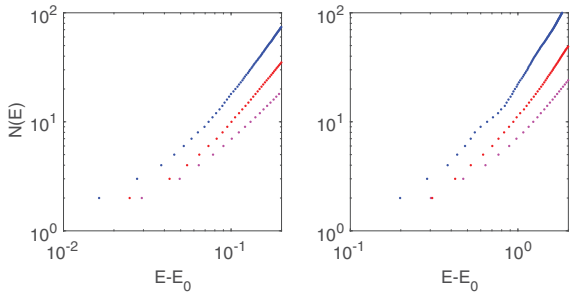

Fig. 7: (Color online) Dependence of the integrated number of states $N(E)$ from ground state E_0 up to energy E for the SYK black-hole regime at $V = 0$ (left panel) and the quantum dot regime $V = \sqrt{14}$ (right panel). Here $M = 14, L = 6, N = 3003$ with average over $N_r = 10$ disorder realizations (blue symbols), $M = 12, L = 5, N = 792, N_r = 38$ (red symbols), $M = 10, L = 4, N = 210, N_r = 150$ (magenta symbols); in all cases $J = 1$. Only the vicinity of ground-state energy is shown.

black hole can be considered as an isolated object with strongly interacting components. Thus, the DTC description of such objects should play an important role for the thermodynamics of black holes proposed in [43].

The extension of the SYK model ($g \ll 1$) to the quantum dot regime ($g > 1$) described by the Hamiltonian (2) raises several new questions. Indeed, excitations at $g > 1$ have an energy gap $\Delta E \propto 1/L^{3/2}$ which drops only algebraically with the number of fermions L. In contrast it is expected that the low energy excitations at $g \ll 1$ have excitation energy $\delta E \propto \exp(-CL)$ which drops exponentially with L (C is some constant). Indeed, the results of fig. 7, showing the average integrated number of states $N(E)$ above the ground energy E_0, confirm that the low excitation energies are by an order of magnitude smaller for $g \ll 1$ compared to the case of $g > 1$. However, much larger values of L and better averaging over many disorder realizations N_r are required to distinguish firmly algebraic and exponential dependences on a number of fermions. At the same time the numerical results for the SYK model with Majorana fermions confirms the exponential drop of δE with L for $g \ll 1$ [19] while the Landau theory of Fermi liquid guarantees an algebraic drop of δE with L for $g \gg 1$. We expect that a quantum phase transition can take place between these two regimes at a certain critical conductance g_c of a quantum dot. The interesting question on the interpretation of negative temperatures for the SYK black holes remains for further studies.

Our results show that quantum dots with moderate conductance values $g \sim 1$ can be close for the SYK black-hole regime. Thus, an experimental investigations of such quantum dots can open new perspectives for studies of the SYK model. Such solid-state systems with $g \ll 1$ have been already studied with a 2D lattice of coupled Sinai billiards [44]. Another possibility to investigate strongly interacting fermions is to consider the regime of Anderson localization where the conductance takes values $g \sim 1$ inside Thouless blocks and interactions are strong near the Fermi level [21,22,45].

Finally extending the suggestion of SYK modeling with cold atoms [8] we propose to consider a case of the Wigner crystal in a periodic potential which, as SYK, is characterized by exponentially small energy excitation inside the pinned Aubry phase [46]. Such an Aubry phase has been recently realized with cold ions in optical lattices [47].

We hope that our results will stimulate further research of duality between SYK black holes and quantum dots with strongly interacting fermions. We note that the dynamical thermalization concept is especially interesting for black holes which can be naturally considered as isolated objects without any contact with a thermostat.

* * *

This research is supported in part by Pogramme Investissements d'Avenir ANR-11-IDEX-0002-02, reference ANR-10-LABX-0037-NEXT (project THETRACOM).

Additional remark: After the submission of this work there appeared a new preprint [48] with additional numerical evidence for exponentially small excitation energies above the SYK ground state.

REFERENCES

[1] Sachdev S. and Ye J., *Phys. Rev. Lett.*, **70** (1993) 3339.
[2] Kitaev A., *A Simple Model of Quantum Holography* (Video talks at KITP Santa Barbara, April 7 and May 27) 2015.
[3] Sachdev S., *Phys. Rev. X*, **5** (2015) 041025.
[4] Polchinski J. and Rosenhaus V., *JHEP*, **2016** (2016) 1.
[5] Maldacena J. and Stanford D., *Phys. Rev. D*, **95** (2016) 106002.
[6] Gu Y., Qi X.-L. and Stanford D., arXiv:1609.07832 [hep-th] (2016).
[7] Gross D. J. and Rosenhaus V., arXiv:1610.01569 [hep-th] (2016).
[8] Danshita I., Hanada M. and Tezuka M., arXiv:1606.02454 [cond-mat.quant-gas] (2016).
[9] Maldacena J., Shenker S. H. and Stanford D., *JHEP*, **2016** (2016) 106.
[10] Bohigas O. and Flores J., *Phys. Lett. B*, **34** (1971) 261.
[11] Bohigas O. and Flores J., *Phys. Lett. B*, **35** (1971) 383.
[12] French J. and Wong S., *Phys. Lett. B*, **33** (1970) 449.
[13] French J. and Wong S., *Phys. Lett. B*, **35** (1971) 5.
[14] Wigner E., *SIAM Rev.*, **9** (1967) 1.
[15] Mehta M. L., *Random Matrices* (Elsevier Academic Press, Amsterdam) 2004.
[16] Bohigas O., Giannoni M. J. and Schmit C., *Phys. Rev. Lett.*, **51** (1984) 1.
[17] Haake F., *Quantum Signatures of Chaos* (Springer, Berlin) 2010.
[18] Ullmo D., *Scholarpedia*, **11** (2016) 31721.
[19] Garcia-Gercia A. M. and Verbaarschot J. J. M., *Phys. Rev. D*, **94** (2016) 126010.

[20] Davidson R. A., Fu W., Georges A., Gu Y., Jensen K. and Sachdev S., arXiv:1612.00849 [cond-mat/str-el] (2016).
[21] Thouless D. J., *Phys. Rev. Lett.*, **39** (1977) 1167.
[22] Akkermans E. and Montambaux G., *Mesoscopic Physics of Electrons and Photons* (Cambridge University Press, Cambridge) 2007.
[23] Åberg S., *Phys. Rev. Lett.*, **64** (1990) 3119.
[24] Åberg S., *Prog. Part. Nucl. Phys.*, **28** (1992) 11.
[25] Jacquod P. and Shepelyansky D. L., *Phys. Rev. Lett.*, **79** (1997) 1837.
[26] Georgeot B. and Shepelyansky D. L., *Phys. Rev. Lett.*, **81** (1998) 5129.
[27] Benenti G., Casati G. and Shepelyansky D. L., *Eur. Phys. J. D*, **17** (2001) 265.
[28] Shepelyansky D. L., *Phys. Scr.*, **T90** (2001) 112.
[29] Sivan U., Milliken F. P., Milkove K., Rishton S., Lee Y., Hong J. M., Boegli V., Kern D. and DeFranza M., *Europhys. Lett.*, **25** (1994) 605.
[30] Gornyi I. V., Mirlin A. D. and Polyakov D. G., *Phys. Rev. B*, **93** (2016) 125419.
[31] Gornyi I. V., Mirlin A. D., Polyakov D. G. and Burin A. L., arXiv:1611.02681 [cond-mat.mes-hall] (2016).
[32] Kolovsky A. R. and Buchleitner A., *EPL*, **96** (2006) 050404.
[33] Flambaum V. V. and Izrailev F. M., *Phys. Rev. E*, **55** (1997) R13.
[34] Nandkishore R. and Huse D. A., *Annu. Rev. Condens. Matter Phys.*, **6** (2015) 15.
[35] D'Alessio, Kafti Y., Polkovnikov A. and Rigol M., *Adv. Phys.*, **65** (2016) 239.
[36] Borgonovi F., Izrailev F. M., Santos L. F. and Zelevinsky V. G., *Phys. Rep.*, **626** (2016) 1.
[37] Landau L. D. and Lifshitz E. M., *Statistical Mechanics* (Wiley, New York) 1976.
[38] Ermann L. and Shepelyansky D. L., *New J. Phys.*, **15** (2013) 123004.
[39] Ermann L., Vergini E. and Shepelyansky D. L., *EPL*, **111** (2015) 50009.
[40] Ermann L., Vergini E. and Shepelyansky D. L., *Phys. Rev. A*, **94** (2016) 013618.
[41] Schlageck P. and Shepelyansky D. L., *Phys. Rev. E*, **93** (2016) 012126.
[42] Abragam A., *The Principles of Nuclear Magnetism* (Oxford University Press, Oxford, UK) 1961.
[43] Bekenstein J. D., *Phys. Rev. D*, **7** (1973) 2333.
[44] Budantsev M. V., Kvon Z. D., Pogosov A. G., Gusev G. M., Portal J. C., Maude D. K., Moshegov N. T. and Toropov A. I., *Physica B*, **256-258** (1998) 595.
[45] Jacquod P. and Shepelyansky D. L., *Phys. Rev. Lett.*, **78** (1997) 4986.
[46] Garcia-Mata I., Zhirov O. V. and Shepelyansky D. L., *Eur. Phys. J. D*, **41** (2007) 325.
[47] Bylinskii A., Gangloff D., Counts I. and Vuletic V., *Nat. Mater.*, **15** (2016) 717.
[48] Garcia-Gercia A. M. and Verbaarschot J. J. M., arXiv:1701.06593 [hep-th] (2017).